

# NUMERICAL CALCULATION OF THE FLOW FIELD IN A BUBBLE COLUMN CONSIDERING THE ABSORPTION OF THE GAS PHASE

**D. Wiemann\*, F. Lehr\*\*, D. Mewes\***

\*Institute of Process Engineering, University of Hannover,  
Callinstraße 36, D-30167 Hannover, Germany  
Phone: +49 511 762-3639, Fax: +49 511 762-3031,  
e-mail: dms@ifv.uni-hannover.de

\*\*Bayer AG, D-51368 Leverkusen, Germany

## ABSTRACT

The interfacial area per unit volume is one of the key parameters for the design of multiphase reactors. In this work a population balance approach is applied to calculate the interfacial area density in a bubble column. The resulting transport equation for the arithmetic bubble volume is coupled with the balance equations for mass and momentum. In addition the physical absorption of the gas phase is considered. The calculations are performed for three dimensional, instationary flow fields in cylindrical bubble columns using the Euler-Euler approach. For the calculation the commercial code CFX-4 is used.

## INTRODUCTION

The interfacial momentum, heat and mass transfer rate in multiphase flows is directly proportional to the interfacial area. Thus the interfacial area density is one of the key parameters for the design of multiphase flow reactors, e.g. tray columns or bubble columns. This paper deals with the numerical calculation of bubbly flow considering the local bubble size distribution. In particular for cylindrical bubble columns the flow field is calculated using an Euler-Euler approach with an additional transport equation for the interfacial area density.

For the calculation of the interfacial area density the amount of bubbles is divided into classes containing bubbles with a volume between  $v_n$  and  $v_n+dv$ . The probability density of bubbles in a certain class

$$f = \frac{N}{V\Delta v} \quad (1)$$

is then defined as the number of bubbles per unit volume and class width. The population balance is the balance equation for  $f$ , thus for each class one equation is required to calculate the bubble size distribution. The total amount of bubbles is thus

calculated as the integral of  $f$ , considering all bubble volumes. In this work the population balance approach following Millies and Mewes [1] is used, see Table 1. The volume of the bubbles within the considered fraction is signed with  $v$  and the volume of bubbles which do not belong to this fraction is signed with  $v'$ . The probability density function is determined by several phenomena. For a certain fraction the probability is increased by a decreasing density of the gas phase, the break-up of larger bubbles and the coalescence of smaller bubbles. In dependence of its direction mass transfer can reduce or increase the probability density. The break-up and coalescence processes are regarded in detail.

*Table 1: Population Balance Equation*

temporal change and convective transport	$\frac{\partial f}{\partial t} + \nabla(\bar{f}\bar{u}_g) =$
changes in the gas density	$+ \frac{1}{\rho_g} \frac{D\rho_g}{Dt} \frac{\partial}{\partial v}(vf)$
mass transfer	$- \frac{\partial}{\partial v} \left( \dot{n}A_p \frac{\mu_g}{\rho_g} f \right)$
break-up of larger bubbles	$+ \int_v^{\infty} r_1(v, v') f(v') dv'$
break-up of bubbles with volume $v$	$- \int_0^v v \dot{n}_1(v, v') dv' \frac{f(v)}{v}$
coalescence of smaller bubbles	$+ \frac{1}{2} \int_0^v r_2(v', v - v') f(v') f(v - v') dv'$
coalescence of bubbles with volume $v$	$- \int_0^{\infty} r_2(v, v') f(v') dv' f(v)$

## BUBBLE BREAK-UP AND COALESCENCE

The probability for the collision of more than two bubbles at the same time is very low compared with the probability for a collision of two bubbles. Thus in this work only binary coalescence processes are considered. For the same reason binary break-up processes are considered. The terms for bubble break-up are calculated in dependence of the break-up kernel function  $r_1(v, v')$

$$r_1(v, v') = \frac{df(v)}{f(v') dv' dt}, \quad (2)$$

which is defined as the number of bubble break-ups per unit time and volume, which lead to the formation of bubble fragments with volume  $v$ .

The coalescence kernel function

$$r_2(v, v') = \frac{df(v - v', v')}{df(v') df(v - v') dt} \quad (3)$$

is defined as the number of bubbles of volume  $v$  which is formed per unit time and volume by the coalescence of two bubbles with volumes  $v_1=v'$  and  $v_2=v-v'$ .

For solving the population balance equation a high numerical effort is necessary, because each fraction requires one equation and the equations are strongly coupled. A partial solution can be derived following the proposal of Millies and Mewes [1]. The integral terms in Table 1 are calculated for the assumption that the kernel functions for break-up and coalescence are independent from  $v'$ . The solution

$$f(v) = \frac{\alpha_g}{\bar{v}^2} \exp\left(-\frac{v}{\bar{v}}\right) \quad (4)$$

results. The arithmetic bubble volume is signed with  $\bar{v}$ . This solution is used to evaluate the population balance equation. The resulting equation only consists of terms with zero or first power of the bubble volume. The mass conservation equation for the gas phase can be derived from the terms with zero power to the bubble volume. The remaining terms of first power are rearranged to the equation

$$\frac{\partial \bar{v}}{\partial t} + \bar{u}_g \nabla \bar{v} = -\frac{1}{\rho_g} \frac{D\rho_g}{Dt} \bar{v} - \frac{\dot{n} a_p}{\alpha_g \rho_g / \mu_g} \bar{v} - \frac{1}{2} r_1 \bar{v}^2 + \frac{1}{2} r_2 \alpha_g. \quad (5)$$

The temporal change and convective transport on the left side are balanced by mass transfer processes and bubble break-up and coalescence. Thus eq. (5) can be interpreted as a transport equation for the arithmetic bubble volume.

The probability of bubble break-up and coalescence is described by the kernel-functions. For modelling these functions the interactions of the bubbles with other bubbles and with the liquid phase are regarded. The phenomena are described by Fan [2] and Fan and Tschuiya [3].

First the bubble break-up is modelled. The bubble break-up is caused by a strong deformation of a bubble in the flow-field due to the turbulent velocity fluctuations in the liquid phase. This deformation leads to a constriction of the bubble and may result in breakage. For modelling the break-up kernel function four assumptions are made:

1. The break-up of bubbles occurs due to the collision of the bubble with eddies of different length-scales (Walter and Blanch [4], Lee, Erickson and Glasgow [5], Luo and Svendsen [6]).
2. In this work only the binary break-up is considered, thus two daughter bubbles are formed by the break-up of a bubble (Walter and Blanch [4], Hesketh, Etchells and Russell [7]).
3. The force equilibrium between the interfacial force of the bubble and the inertial force of the eddy rules the bubble break-up (Levich [8]). Breakage occurs, if the inertial force of the eddy is higher than the superficial force of the bubble. Assuming a cylindrical constriction the force equilibrium at the smaller daughter bubble is

$$\frac{1}{2} \rho_l u_\lambda^2 = 2 \frac{\sigma}{d'} \quad (6)$$

with the turbulent velocity of the eddy  $u_\lambda$ .

4. The length-scale of the eddy  $\lambda$  must be smaller than the bubble to induce breakage. Greater eddies only transport the bubble (Lee, Erickson and Glasgow [5], Luo and Svendsen [6], Prince and Blanch [9]).

Also the diameter of the smaller daughter bubble must be smaller than the eddy, thus

$$d' \leq \lambda \leq d. \quad (7)$$

The kernel functions for bubble break-up and coalescence are modelled following Lehr and Mewes [10], thus it is written

$$r_1(v, v') = \int \frac{d}{d'} \sqrt{2} C \frac{\sigma}{\rho_l \varepsilon^{2/3} d'^4} \frac{(\lambda + d)^2}{\lambda^{13/3}} \exp\left(-\frac{2\sigma}{\rho_l \varepsilon^{2/3} d'} \frac{1}{\lambda^{2/3}}\right) d\lambda, \quad (8)$$

$$C = 0.8413$$

For the coalescence process the following assumptions are made:

1. Two bubbles (indices 1 and 2) collide, thus only binary coalescence processes are considered.
2. The collision occurs due to turbulent velocity fluctuations or due to different rise velocities of the bubbles. The characteristic velocity for the coalescence process is therefore the relative velocity between the bubbles or the turbulent eddy velocity.
3. Coalescence only occurs if the characteristic velocity is lower than a certain critical value. Otherwise the bubbles bounce. This critical value is determined for water-air to  $u_{crit}=0.08$  m/s.

Following Lehr and Mewes [10] the coalescence kernel function is written

$$r_2(v_1, v_2) = \frac{\Pi}{4} (d_1 + d_2)^2 \min(u', u_{crit}) \quad (9)$$

with the characteristic velocity

$$u' = \max\left[\sqrt{2}(\varepsilon \sqrt{d_1 d_2})^{1/3}; |\bar{u}_1 - \bar{u}_2|\right] \quad (10)$$

The population balance equation given in Tab.1 is evaluated numerically for certain values of  $\varepsilon, \alpha$  and different material properties using eqs. (8) and (9). The results are given in Fig. (1). The dimensionless probability density is expressed in dependence of the arithmetic bubble volume by a lognormal distribution

$$\hat{f} := \frac{\bar{v}^2}{\alpha_g} f = \sqrt{\frac{2}{\Pi}} \frac{\bar{v}}{3v} \exp\left[-\frac{2}{9} \ln\left(e^{-9/8} \frac{v}{\bar{v}}\right)\right]. \quad (11)$$

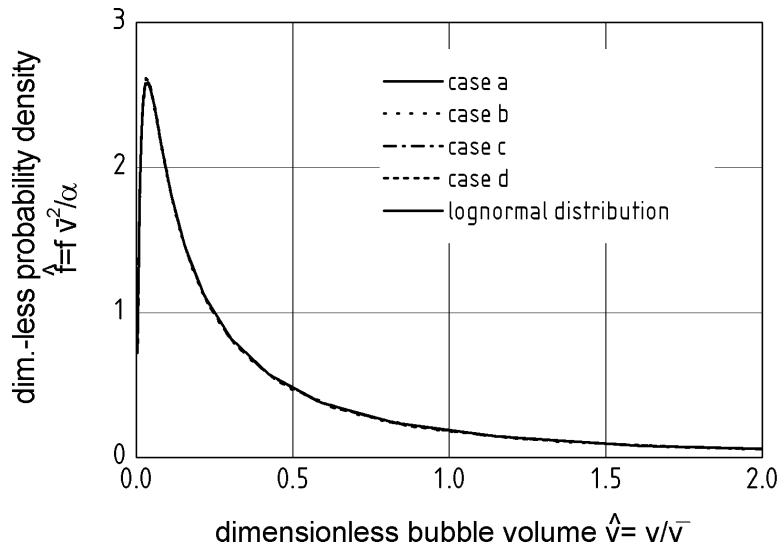


Figure 1: Dimensionless bubble size distribution

- case a:  $\rho_l=998.0 \text{ kg/m}^3$ ,  $\sigma=0.0727 \text{ kg/s}^2$ ,  $\alpha_g=0.25$ ,  $\varepsilon=2.0 \text{ m}^3/\text{s}^2$   
case b:  $\rho_l=998.0 \text{ kg/m}^3$ ,  $\sigma=0.0727 \text{ kg/s}^2$ ,  $\alpha_g=0.4$ ,  $\varepsilon=4.0 \text{ m}^3/\text{s}^2$   
case c:  $\rho_l=998.0 \text{ kg/m}^3$ ,  $\sigma=0.02 \text{ kg/s}^2$ ,  $\alpha_g=0.25$ ,  $\varepsilon=2.0 \text{ m}^3/\text{s}^2$   
case d:  $\rho_l=500.0 \text{ kg/m}^3$ ,  $\sigma=0.02 \text{ kg/s}^2$ ,  $\alpha_g=0.25$ ,  $\varepsilon=2.0 \text{ m}^3/\text{s}^2$

Thus the bubble size distribution can be calculated if the arithmetic bubble volume and the volume fraction are known.

## MASS TRANSFER

The mass transfer from the gas into the liquid phase is considered due to the physical absorption of the gas phase. The mass transfer rate per unit interfacial area

$$\dot{m}_{g,l} = \beta_l (\rho_{\text{CO}_2,pl}^* - \rho_{\text{CO}_2,l}) \quad (12)$$

is calculated in dependence of the liquid mass transfer coefficient and the partial density of  $\text{CO}_2$ . The mass transfer resistance is assumed only in the liquid phase. The concentration in the liquid away from the phase interface is assumed to be constant. At the phase interface the partial density  $\rho_{\text{CO}_2,l}^*$  is calculated following Henry's law. The physical absorption of  $\text{CO}_2$  into water is investigated experimentally for single bubbles by Hallensleben [11]. The mass transfer coefficients are shown in Fig. (2). In addition the calculated values following Higbie's theory are given.

For small bubbles the inhibition of the interfacial motion reduces the mass transfer rate. For larger bubbles the experimental results approach the theoretical values.

Following Hallensleben the mass transfer coefficient for single bubbles in the range of  $2\text{mm} < d < 6\text{mm}$  is approximately constant

$$\beta_l = 0.00028 \text{ m/s}. \quad (13)$$

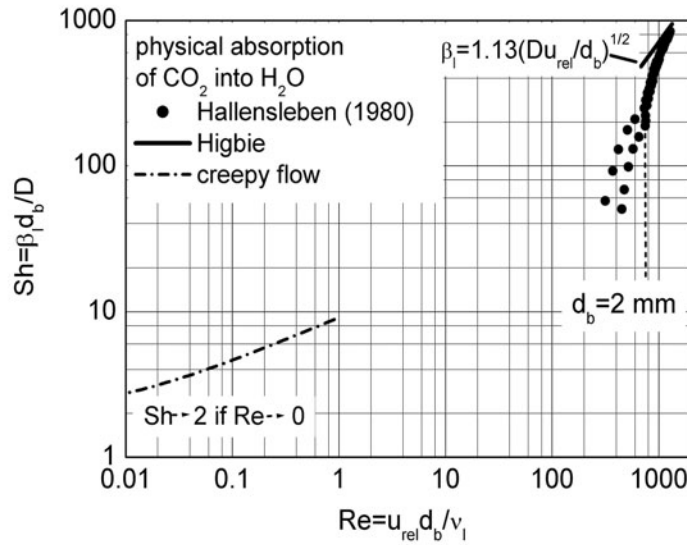


Figure 2: Sh-number in dependence of Re-number for bubbles

The mass transfer coefficient for a bubble within a bubble swarm is of the same order as for a single bubble following Hallensleben.

## NUMERICAL CALCULATION

For the numerical calculation a two-fluid Euler-Euler approach is used to describe the gas and the liquid phase. Both phases are treated as quasi-continuous. Thus the mass balance equation for each phase is written as

$$\frac{\partial(\alpha_i \rho_i)}{\partial t} + \nabla(\alpha_i \rho_i \bar{u}_i) = \pm \dot{M}_{g,l}; i = g, l. \quad (14)$$

The mass transfer rate from the gas into the liquid phase is labelled  $\dot{M}_{g,l}$ , thus the minus sign is used for the gas phase. The momentum balance equation is

$$\frac{\partial(\alpha_i \rho_i \bar{u}_i)}{\partial t} + \nabla(\alpha_i [\rho_i \bar{u}_i \bar{u}_i - \eta_i (\nabla \bar{u}_i + \nabla \bar{u}_i^T)]) = -\alpha_i \nabla p + \bar{F}_p + \alpha_i \rho_i \bar{g} \quad (15)$$

The interphase momentum transfer is modelled by the transfer terms  $\bar{F}_p$ . The turbulent velocity fluctuations in the liquid phase are modelled using a k- $\epsilon$ -turbulence model with additional source terms including bubble-induced turbulence. The transport equation for the arithmetic bubble volume is implemented into the commercial CFD-code CFX-4. The interphasial transfer terms for mass and momentum are calculated in dependence of it.

The Euler-Euler approach is used particularly in regard to the performance of the present computers. The alternative Euler-Lagrange approach, which requires one momentum balance for each bubble, is presently inapplicable for a bubble swarm. Nevertheless for the later discussed absorption process of CO<sub>2</sub> the calculation of 10 s takes 1 day on a Sun Blade 1000 workstation.

## RESULTS AND DISCUSSION

The calculations are performed for instationary, three-dimensional flow fields in cylindrical bubble columns. The basic influence of mass transfer to the flow field in a bubble column is shown in [Fig. 3](#). For this purpose the flow field for the system water-air has been calculated assuming a constant amount of gas is transferred into the liquid per unit interfacial area. In addition the case without mass transfer is given.

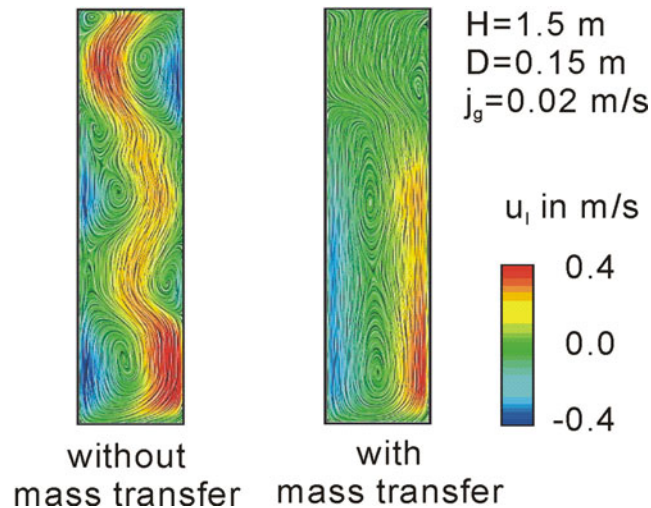


*Figure 3: Basic influence of mass transfer to the flow field*

The momentum transfer from the gas phase to the liquid phase is reduced significantly due to the absorption process. As a consequence the amount of vortices is diminished in particular in the upper part of the column. The backflow of the liquid phase is enhanced by the formation of a recirculation pattern in the lower part of the column.

For the further investigations the system CO<sub>2</sub>-water is chosen, because of the high solubility of CO<sub>2</sub> in water. Therefore the experimental investigations of Hillmer [12] are taken as reference. The column has a diameter of D=0.19 m and a height of H=2.80 m. The superficial velocity is of  $j_g=0.02$  m/s for the gas phase and  $j_l=0.05$  m/s for the liquid phase. The initial bubble size at the distributor is assumed to d=0.004 m in accordance to the experimental investigations of Hillmer [12].

In [Fig. 4](#) the calculated bubble diameter and volume fraction of gas are shown for different cross sectional areas. The instantaneous bubble diameter increases due to coalescence processes in the lower part of the column and decreases due to the absorption process in the upper part.

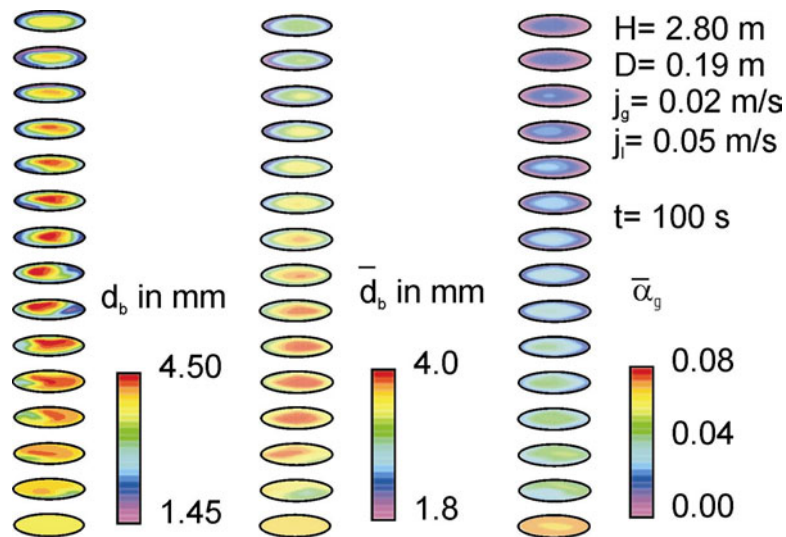


Figure 4: Bubble diameter and volume fraction

The time averaged bubble diameter decreases with the column height, except of the region next to the sparger, where the bubbles growth due to coalescence processes. The time averaged volume fraction decreases with the column height. In particular the volume fraction is reduced in the lower part of the column. The instantaneous velocity field of the liquid phase and the instantaneous volume fraction of gas are shown in Fig. 5. The volume fraction of gas is shown within two longitudinal sections with an angle of  $90^\circ$  between them. The streamlines of the liquid phase are visualised by a texture.

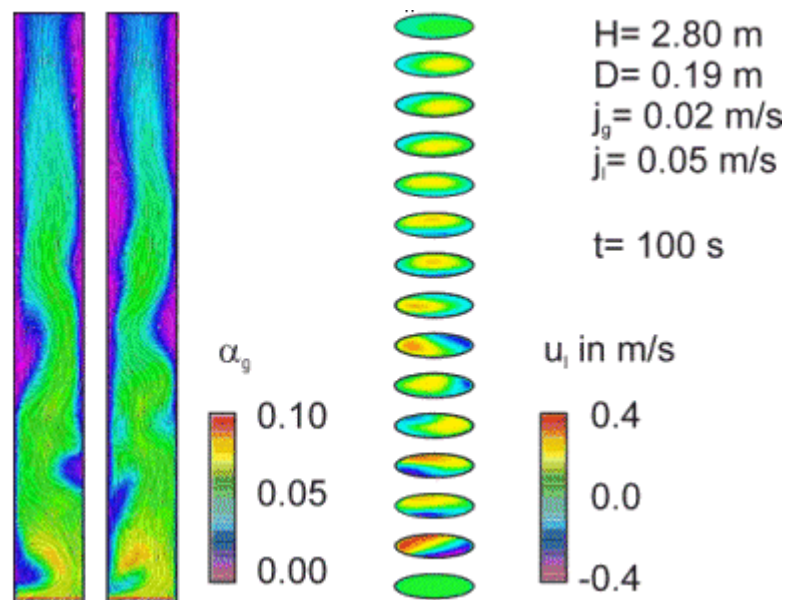


Figure 5: Instantaneous flow field

The instantaneous flow field of the liquid phase is characterized by vortices in the lower part of the column. The amount of vortices is reduced with the column height. The absorption of the gas with the column height lowers the vertical velocity of the liquid phase, thus the variation of the liquid velocity in a cross section is reduced, too.



In Fig. 6 the area weighted gas flow rate is shown as a function of the column height. The calculated gas flow rate is time averaged over 10 s to diminish the influence of axial velocity fluctuations.

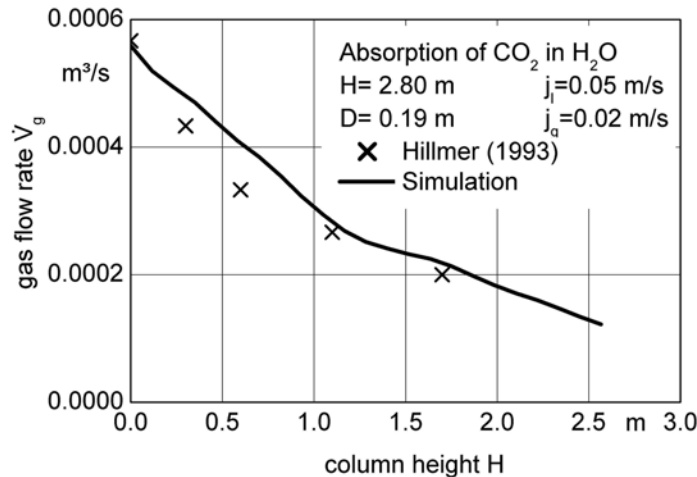


Figure 6: Flow rate of gas with the column height

In addition the experimental investigations from Hillmer [12] are depicted. The gas flow rate at the outlet is about 18 per cent of the initial flow rate at the inlet. In particular the gas flow rate is reduced in the lower half of the column.

## CONCLUSION

A population balance approach is applied to bubble columns to calculate the local interfacial area density. The bubble break-up and coalescence processes are considered. In dependence of the local flow field the arithmetic bubble volume is calculated, thus the interfacial area is known. For the system CO<sub>2</sub>–water the absorption of the gas phase is considered. Therefore a constant mass transfer coefficient is assumed following the experimental investigations of Hallensleben. In the lower part of the column the velocity field of the liquid is characterized by vortices, whereas in the upper part the liquid rises up straightforward. Thus in the lower part of the column the residence time for the bubbles is longer than in the upper part.

## ACKNOWLEDGEMENT

The authors gratefully acknowledge the financial support of the “German Research Foundation” (DFG).

## NOMENCLATURE

A	[m <sup>2</sup> ]	surface area of a bubble
a	[1/m <sup>3</sup> ]	interfacial area density
D	[m]	bubble column diameter
d	[m]	bubble diameter
f	[1/m <sup>6</sup> ]	number density
H	[m]	bubble column height
j	[m/s]	superficial velocity
k	[m <sup>2</sup> /s <sup>2</sup> ]	turbulent kinetic energy
N	[-]	number
n	[1/m <sup>3</sup> ]	number density
$\dot{n}$	[kmol/	molar flux
r1	[1/m <sup>3</sup> /s]	break-up kernel function
r2	[m <sup>3</sup> /s]	coalescence kernel
u	[m/s]	velocity component
$\vec{u}$	[m/s]	velocity vector
u <sub>crit</sub>	[m/s]	critical velocity for
u'	[m/s]	turbulent fluctuating
v	[m <sup>3</sup> ]	bubble volume
$\bar{v}$	[m <sup>3</sup> ]	average bubble volume

## Greek symbols and Indices

$\alpha$	[-]	volume fraction
$\beta$	[m/s]	mass transfer coefficient
$\varepsilon$	[m <sup>2</sup> /s <sup>3</sup> ]	dissipation rate
$\lambda$	[m]	length scale of an eddy
$\sigma$	[kg/s <sup>2</sup> ]	surface tension
$\rho$	[kg/m <sup>3</sup> ]	density

l liquid

g gas

t turbulent

' daughter bubble

\* dimensionless

p interfacial

## REFERENCES

1. M. Millies and D. Mewes (1996), Chem. Ing. Tech., 68, 660-669
2. L. S. Fan (1989), Gas-Liquid-Solid fluidization engineering, Butterworth, Stoneham, MA
3. L. S. Fan and K. Tsuchiya (1990), Bubble wake dynamics in liquids and liquid-solid suspensions, Butterworth, Stoneham, MA
4. J. F. Walter and H. Blanch (1986), Chem. Eng. J., 32, B7-B17
5. C. H. Lee, L. E. Erickson and L. A. Glasgow, L. A. (1987), Chem. Eng. Com., 59, 65-84
6. H. Luo and H. F. Svendsen (1996), AIChE J., 42, 1225-1233
7. R. P. Hesketh and A. W. Etchells and T. W. F. Russell (1991), Chem. Eng. Sci., 46, 1-9
8. Levich, V. G., 1962, "Physicochemical Hydrodynamics", PrenticeHall, N. J.
9. M. J. Prince and H. W. Blanch (1990), AIChE J., 36, 1485-1499
10. F. Lehr and D. Mewes (2001), Chem. Eng. Sci. 56, 1159-1166
11. J. Hallensleben (1980), Simultaner Stoffaustausch von CO<sub>2</sub> und Sauerstoff an Einzelblasen und in Blasenschwärmen, PhD thesis, University of Hannover, Germany
12. G. Hillmer (1993), Experimentelle Untersuchung und Modellierung von Suspensionsblasensäulen, PhD thesis, University of Erlangen-Nürnberg, Germany